JOURNAL OF THE AMERICAN COLLEGE OF CARDIOLOGY
© 2015 BY THE AMERICAN COLLEGE OF CARDIOLOGY FOUNDATION
PUBLISHED BY ELSEVIER INC.
VOL. 66, NO. 2, 2015
ISSN 0735-1097/$36.00
http://dx.doi.org/10.1016/j.jacc.2015.04.064

Heme Oxygenase-1 Gene Therapy Provides Cardioprotection Via Control of Post-Ischemic Inflammation

An Experimental Study in a Pre-Clinical Pig Model

Rabea Hinkel, DVM,*†‡ Philipp Lange, MD,* Björn Petersen, DVM,§ Elena Gottlieb, MD,* Judy King Man Ng, PhD,*‡ Stefanie Finger, MSc,‖ Jan Horstkotte, MD,* Seungmin Lee, MSc,* Michael Thormann, DVM,* Maike Knorr, MD,‖ Chiraz El-Aouni, PhD,* Peter Boekstegers, MD,* Bruno Reichart, MD,¶ Philip Wenzel, MD,‖ Heiner Niemann, DVM,§ Christian Kupatt, MD*‡¶

ABSTRACT

BACKGROUND Heme oxygenase-1 (HO-1) is an inducible stress-responsive enzyme converting heme to bilirubin, carbon monoxide, and free iron, which exerts anti-inflammatory and antiapoptotic effects. Although efficient cardioprotection after HO-1 overexpression has been reported in rodents, its role in attenuating post-ischemic inflammation is unclear.

OBJECTIVES This study assessed the efficacy of recombinant adenoassociated virus (rAAV)-encoding human heme oxygenase-1 (hHO-1) in attenuating post-ischemic inflammation in a murine and a porcine ischemia/reperfusion model.

METHODS Murine ischemia was induced by 45 min of left anterior descending occlusion, followed by 24 h of reperfusion and functional as well as fluorescent-activated cell sorting analysis. Porcine hearts were subjected to 60 min of ischemia and 24h of reperfusion before hemodynamic and histologic analyses were performed.

RESULTS Human microvascular endothelial cells transfected with hHO-1 displayed an attenuated interleukin-6 and intercellular adhesion molecule 1 expression, resulting in reduced monocytic THP-1 cell recruitment in vitro. In murine left anterior descending occlusion and reperfusion, the post-ischemic influx of $CD45^+$ leukocytes, $Ly\text{-}6G^+$ neutrophils, and $Ly\text{-}6C^{high}$ monocytes was further exacerbated in HO-1-deficient hearts and reversed by rAAV.hHO-1 treatment. Conversely, in our porcine model of ischemia, the post-ischemic influx of myeloperoxidase-positive neutrophils and $CD14^+$ monocytes was reduced by 49% and 87% after rAAV.hHO-1 transduction, similar to hHO-1 transgenic pigs. Functionally, rAAV.hHO-1 and hHO-1 transgenic left ventricles displayed a smaller loss of ejection fraction than control animals.

CONCLUSIONS Whereas HO-1 deficiency exacerbates post-ischemic cardiac inflammation in mice, hHO-1 gene therapy attenuates inflammation after ischemia and reperfusion in murine and porcine hearts. Regional hHO-1 gene therapy provides cardioprotection in a pre-clinical porcine ischemia/reperfusion model. (J Am Coll Cardiol 2015;66:154–65)

From the *Medizinische Klinik I, Klinikum Grosshadern, Ludwig Maximilian University, Munich, Germany; †Institute for Cardiovascular Prevention, Ludwig Maximillian University, Munich, Germany; ‡Medizinische Klinik I, Klinikum Rechts der Isar, Technical University of Munich, and German Center for Cardiovascular Research, partner site Munich Heart Alliance, Munich, Germany; §Institute of Farm Animal Genetics, Friedrich-Loeffler-Institut, Mariensee, Germany; ‖Department of Medicine 2, Center for Thrombosis and Hemostasis Mainz and German Center for Cardiovascular Research, partner site Rhine Main, Mainz, Germany; and the ¶Walter-Brendel-Centre for Experimental Medicine, Munich, Germany. This study was funded by the German Research Foundation (SFB-TRR 127 to Drs. Hinkel, Petersen, Reichart, Niemann, and Kupatt), the German Center for Cardiovascular Research, the German Ministry for Education and Research (01EO1003 to Dr. Wenzel, BMBF01GU1105 to Dr. Kupatt), and an institutional grant of the Klinikum to Dr. Gottlieb (FöFoLe). The authors have reported that they have no relationships relevant to the contents of this paper to disclose. Drs. Hinkel, Lange, and Petersen contributed equally to this work.
Listen to this manuscript's audio summary by *JACC* Editor-in-Chief Dr. Valentin Fuster.

Manuscript received February 6, 2015; revised manuscript received April 1, 2015, accepted April 13, 2015.

Heme proteins, such as mammalian hemoglobin and myoglobin, are central to oxygen transport and storage. However, with an ischemic crisis, heme protein catabolism may become crucial to avoid accumulation of heme, a proinflammatory damage signal (1). Coincidentally, heme catabolism produces biliverdin, a potential scavenger of reactive oxygen species, and carbon monoxide, which modulates excessive inflammatory activation (2).

SEE PAGE 166

Accordingly, previous evidence suggests that heme oxygenase-1 (HO-1) may serve as a therapeutic agent in case of myocardial infarction. In rats, transduction of a wild-type adenoassociated virus (AAV) 2 vector encoding for human heme oxygenase-1 (hHO-1) ameliorated post-ischemic remodeling and function over 12 months of chronic ischemia inflicted by permanent coronary occlusion (3) as well as repetitive ischemia models (4). Moreover, HO-1-transgenic (tg) mice displayed less cardiomyocyte loss and left ventricular (LV) impairment after chronic left anterior descending (LAD) artery occlusion than nontransgenic control mice (5). Thus, HO-1 improves late cardiac remodeling post-infarction by regenerative monocytes (6) and fibroblasts (7).

In contrast, acute ischemia and reperfusion (I/R) implies an enhanced variant of post-ischemic inflammation caused by reperfusion-related rapid influx of well-oxidized blood carrying damaging inflammatory cells to the central ischemic area. Damage-associated molecular patterns from the injured myocardium and extracellular matrix activate membrane-bound toll-like receptors (TLR), inducing a proinflammatory state in cardiomyocytes and adjacent endothelial cells in concert with extracellular reactive oxygen species (8,9). Neutrophils are recruited to acutely activated endothelium as inflammatory first responders, subsequently transmigrating to the myocyte compartment and exerting tissue damage via myeloperoxidase (MPO) and proteolytic enzymes (10). This cytotoxic effect may add to infarct expansion by overwhelming inflammation (9), in particular in scenarios of I/R, which reestablishes central perfusion of the necrotic core distal to the occlusion site. Moreover, neutrophils actively induce the subsequent phagocytotic phase of inflammation (11), mediated by monocytes and macrophages, to allow for the later repair phase and resolution of inflammation (9). This time course of inflammation is mirrored by a sequence of predominant inflammatory cell subsets in murine hearts: Ly-6G^{+} neutrophils give way to Ly-6C^{high} monocytes, which are followed by angiogenic and regenerative Ly-6C^{low} monocytes (12).

Although modulation of early post-ischemic inflammation may limit infarct expansion, targeting leukocyte recruitment is notoriously difficult because of the high redundancy of inflammatory systems (13). Conversely, attenuation of the early cytotoxic phase of post-ischemic inflammation seems an attractive target, which HO-1 may readily provide. This notion is supported by the reduction in cluster of differentiation (CD) 45^{+} cell invasion in histological samples of HO-1.tg mice subjected to I/R (14).

However, the effect of HO-1 on proinflammatory or regenerative leukocyte subsets recruited to the post-ischemic heart has not yet been investigated. In human or porcine models, MPO-positive (MPO^{+}) cells represent murine Ly-6G^{+} neutrophils, whereas CD14^{high} cells resemble proinflammatory monocytes and CD14^{-} CD16^{+} monocytes may constitute the proangiogenic population (12). Because HO-1 has been reported to inhibit leukocyte adhesion during inflammation in the heart (15) and other organs (16), we sought to investigate its role in modulating I/R inflammation in murine and porcine myocardial I/R models.

METHODS

Recombinant rAAV.hHO-1 was produced using the triple transfection method as described previously (17). Human microvascular endothelial cells (HMECs) were activated by lipopolysaccharide, 200 ng/ml for 6 h; then either supernatant was assessed for interleukin-6 secretion by enzyme-linked immunosorbent assay (R&D Systems, Inc., Wiesbaden, Germany) or cells were incubated with an intercellular adhesion molecule-1 antibody (sc-1511, Santa Cruz Biotechnology, Inc., Heidelberg, Germany) and a secondary antibody (sc-2014, Santa Cruz) before fluorescent-activated cell sorting analysis.

Ibidi-slides (ibiTreat VI0.4, Martinsried, Germany) were seeded with HMECs pre-treated either with lipofectamine-coated plasmids for empty backbone (pcDNA) or hHO-1, with or without coapplication of the HO-1 blocker zinc protoporphyrin (ZnPP). After 24 h, when cell layer was confluent, human umbilical vein endothelial cells were stimulated with lipopolysaccharide, 200 ng/ml or high mobility group box 1, 5 μg/ml for 1.5 h. Then, THP-1 monocytic cells were superfused at a concentration of 750,000 cells/ml and at a shear rate of 0.57 ml/min

ABBREVIATIONS AND ACRONYMS

AAR = area at risk
CD = cluster of differentiation
EF = ejection fraction
hHO = human heme oxygenase
HMEC = human microvascular endothelial cell
HO = heme oxygenase
I/R = ischemia and reperfusion
LAD = left anterior descending
LV = left ventricular
MPO = myeloperoxidase
rAAV = recombinant adenoassociated virus
tg = transgenic
TLR = toll-like receptor
WMSI = wall motion score index
ZnPP = zinc protoporphyrin

(=1 dyne/cm^2) (Harvard Apparatus, Holliston, Massachusetts). After 8 min of cell superfusion and 1 min of washing with medium only, adherent cells were counted.

Myocytic HL-1 cells and HMECs were cultivated in Claycomb medium or Dulbecco's modified Eagle medium (plus 10% fetal calf serum, plus 1% penicillin/streptomycin), respectively. HL-1 cells were transfected using Satisfection (TPP AG, Trasadingen, Switzerland) according to the manufacturer's protocol. Then, 48 h later, hHO-1-transfected cells were plated on 24-well plates to undergo 18 h of hypoxia (1% oxygen) followed by 4 h of reoxygenation. Cell death was assessed via trypan blue staining. Results are given as percentage of living cells.

Total ribonucleic acid was extracted from the control group, rAAV.hHO-1, and the hHO-1.tg groups, treated with DNaseI (Invitrogen, Darmstadt, Germany) and converted to complementary DNA. Quantitative real-time polymerase chain reaction was performed with primer pairs for hHO-1.

Animal care and all experimental procedures were performed in accordance with the Animal Care and Use Committees of Bavaria, Rhineland-Palatinate, and Lower Saxony, Germany. All pig experiments were conducted at the Walter-Brendel Centre for Experimental Medicine at the Ludwig Maximilian University Munich and the Center for Thrombosis and Hemostasis, University Medical Center Mainz.

Male C57BL/6, TLR4$^{-/-}$ on C57BL/6 background as well as HO-1$^{+/+}$, HO-1$^{+/-}$, and HO-1$^{-/-}$ mice (18) on a mixed C57BL/6/129sv/Balb-C background (8 to 12 weeks old) underwent either myocardial I/R injury or sham operation. A total of 5×10^{12} virus particles of an rAAV-encoding hHO-1 were injected into the tail vein 14 days before further instrumentation, where indicated (Online Figure 1A). Mice were anesthetized and mechanically ventilated. Ischemia injury was induced by occlusion of the LAD coronary artery with an 8-0 polypropylene suture. After ischemic injury for 45 min, the occluding suture was opened and the myocardium reperfused for 24 h. Sham mice underwent the same procedure but without coronary artery ligation.

Reperfusion was then allowed for 24 h, followed by echocardiographic monitoring (Vevo 770 and 2100, VisualSonics, Inc., Toronto, Canada; n = 20 per group). Parasternal long-axis views were obtained for assessment of ejection fraction (EF). Validation of the wall motion score index (WMSI) was adapted from Zhang et al. (19). An 11-segment model of WMSI based on 1 parasternal long-axis B-mode view (5 segments: apical, mid-anterior, mid-inferior, basal-anterior, basal-inferior) and 1 mid-ventricular parasternal short-axis B-mode view (6 segments: anteroseptal, anterior, anterolateral, inferolateral, inferior, inferoseptal) was calculated. Wall motion was scored 1 for normal, 2 hypokinetic, and 3 akinetic. WMSI was assessed as the sum of all scores divided through the amount of evaluated segments. Wall motion was considered abnormal at WMSI >1.4.

In a different set of experiments (n = 6 per group), pinhole single-photon emission computerized tomography measurement of infarct size (20) was conducted 45 min after injection of 200 μl [99mTc]-sestamibi (370 MBq, Cardiolite, Bristol-Myers Squibb Medical Imaging Inc., Munich, Germany) via tail vein. Mice were positioned in the center field of the gamma camera and scanned for 30 min.

Invasive monitoring of LV function was performed under intravenous anesthesia (n = 7 per group) with a pressure tip catheter (Millar, Inc., Houston, Texas). The catheter was advanced through the left carotid artery and aorta into the LV under continuous monitoring of the pressure curves until the diastolic pressure indicated localization in the LV (21).

Ten-milligram pieces of post-ischemic hearts were digested with collagenase II (1 mg/ml)/DNase (50 μg/ml), pressed through a cell strainer (70 μm), and centrifuged at 300 *g*. After discarding the supernatant, red blood cells were lysed with an ammonium-potassium buffer, washed twice, and stained for viability (trypan blue). After resuspension of the cell pellet and unspecific Fc binding blockade (2% fetal calf serum, CD16/32), cells were stained with specific antibodies for CD45.2, CD11b, CD3, Ly-6C, and Ly-6G for 15 min, washed twice, and transferred to fluorescent-activated cell sorting tubes.

hHO-1.tg pigs were generated as described previously (22). Cloned syngenic offspring were used for the acute myocardial infarction pig model (Online Figures 1B and 2).

Twenty-one days before I/R injury, the myocardium was transduced with hHO-1 by selective pressure regulated retroinfusion of 1×10^{13} rAAV.hHO-1 particles into the anterior ventricular vein, which anatomically drains the LAD-perfused myocardium (23,24). Three weeks later, the I/R injury protocol was performed.

Pigs (n = 5 per experimental group) were anesthetized. Access to vessels and catheterization were performed as previously described (25).

EF and LV end-diastolic pressure measurements were performed before ischemia and after 24 h of reperfusion. Additionally, regional myocardial function was obtained at 24 h of reperfusion via ultrasound crystals (Sonometrics Corporation, Ontario, Canada).

FIGURE 1 hHO-1 Limits Inflammatory Activation of Endothelial Cells

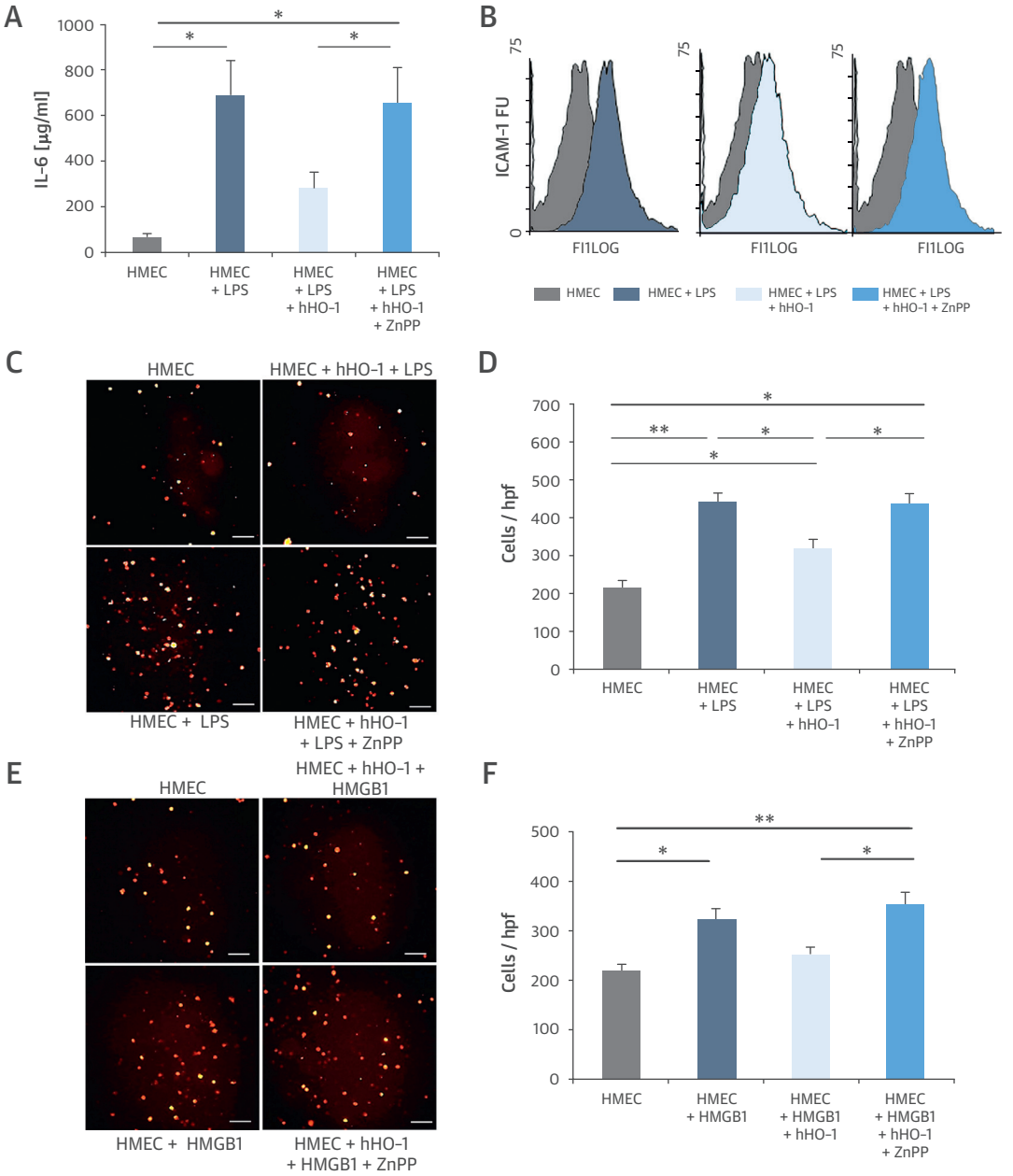

(A) Lipopolysaccharide (LPS)-induced interleukin (IL)-6 production in cultured endothelial cells, which was reduced after human heme oxygenase-1 (hHO-1) transfection, unless the HO-1 inhibitor zinc protoporphyrin (ZnPP) was coapplied. **(B)** The leukocyte adhesion molecule intercellular adhesion molecule (ICAM)-1 was up-regulated by LPS, whereas hHO-1 overexpression attenuated the response. ZnPP blocked the effect of hHO-1. Examples **(C)** and quantitative analysis **(D)** of THP-1 cell adhesion under venular shear stress (1 dyne/s, scale bar 100 µm), which was increased after LPS; hHO-1-transfection reduced THP-1 adhesion, unless inhibited by ZnPP. **(E and F)** High mobility group box 1 (HMGB1) induced a similar proadhesive effect, which was attenuated by hHO-1. Mean ± standard error of the mean; n = 5; *$p < 0.05$, **$p < 0.001$. HMEC = human microvascular endothelial cells; hpf = high-power field.

FIGURE 2 Effect of HO-1 on Murine Post-Ischemic Inflammation

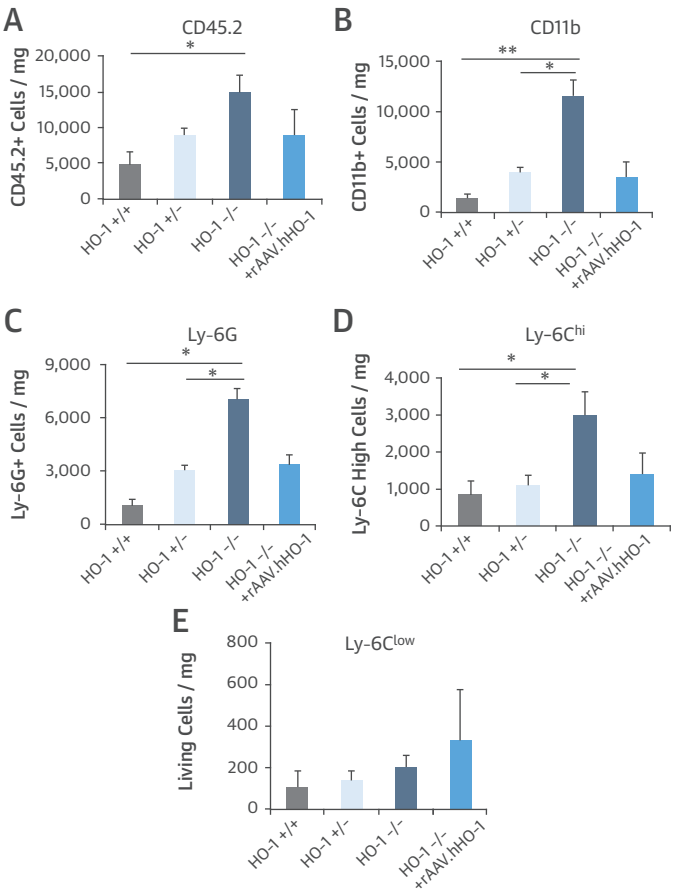

HO-1$^{-/-}$ hearts, ischemia (45 min), and reperfusion (24 h) increased recruitment of CD45.2^{+} **(A)**, CD11b^{+} **(B)**, Ly-6G^{+} neutrophilic **(C)**, and Ly-6C^{high} **(D)** proinflammatory monocyte cells, compared with HO-1$^{+/+}$ hearts. These alterations were attenuated by application of recombinant adenoassociated virus (rAAV)-encoding hHO-1. **(E)** No difference was found in Ly-6C^{low} monocytes between groups. Mean ± standard error of the mean; n = 7; *p < 0.05, **p < 0.001. Abbreviations as in Figure 1.

Subendocardial segment shortening was assessed in the ischemic and nonischemic region at rest and under increased heart rate (120 and 150 beats/min).

Infarct size was assessed via methylene blue exclusion and tetrazolium red viability staining (26). Before explantation of the heart, the LAD was ligated at the site of infarct induction and methylene blue injected into the LV. After excision of the heart tissue samples of the infarct area, the area at risk (AAR), and the control region were harvested for terminal deoxynucleotidyltransferase dUTP nick end labeling assay, capillary staining, viability staining (tetrazolium red), and CD14-staining, as well as MPO assay.

The MPO assay was performed for evaluation of leukocyte influx in the ischemic area (AAR and infarct) (27). Tissue from the AAR was analyzed for capillary density (PECAM-1, Santa Cruz) staining of slices 2 and 3 (23). Apoptosis detection (ApopTag Kit, Millipore, Schwalbach, Germany) was done according to the manufacturer protocol in the ischemic AAR and the nonischemic control area. Nuclei were counterstained with 4′,6-diamidino-2-phenylindole (Vector Laboratories, Burlingame, California).

STATISTICAL METHODS. The results are given as mean ± SEM. Statistical analyses were performed via 1-way analysis of variance. When a significant effect was obtained with analysis of variance, usually the multiple comparison test between the groups with the Student-Newman-Keuls test was performed. However, for WMSI analysis, the nonparametric Kruskal-Wallis test was used. For the interleukin-6 enzyme-linked immunosorbent assay and the apoptosis index, Dunnett-T3 test was used because of the variance heterogeneity. A p value <0.05 was considered significant.

RESULTS

To determine whether HO-1 would affect endothelial activation during post-ischemic inflammation, we assessed inflammatory activation and function of HMEC. We found that inflammatory stimulation of endothelial cells resulted in increased expression of cytokines, such as interleukin-6 (**Figure 1A**), and adhesion molecules, such as intercellular adhesion molecule-1 (**Figure 1B**). Plasmid transfection of hHO-1 blunted expression of both inflammatory proteins. Moreover, recruitment of monocytic THP-1 cells was analyzed in vitro under venular shear stress, such as occurring during firm adhesion in vivo (28). Here, hHO-1 decreased the number of THP-1 cells adhering on human endothelial cells after stimulation with lipopolysaccharide (**Figures 1C and 1D**), as well as high mobility group box 1 (**Figures 1E and 1F**).

To assess the impact of HO on post-ischemic inflammation in vivo, we first compared HO-1-deficient mice and wild-type siblings, which were subjected to 45 min of LAD ligation and 24 h of reperfusion (Online Figure 1A). There was a 3-fold increase of CD45.2^{+} leukocytes into the ischemic area in HO-1-deficient mice compared with control animals (14.9 ± 3.6 × 10^3 vs. 4.8 ± 1.8 × 10^3 cells/mg tissue, respectively) (**Figure 2A**). CD11b^{+} leukocytes were increased more than 6-fold in HO-1$^{-/-}$ hearts (10.0 ± 2.3 × 10^3 cells/mg) than in control animals (1.6 ± 0.3 × 10^3 cells/mg), with HO-1 heterozygous hearts displaying an intermediate level (3.9 ± 0.5 × 10^3 cells/mg)

FIGURE 3 Effect of HO-1 in Murine Ischemia and Reperfusion

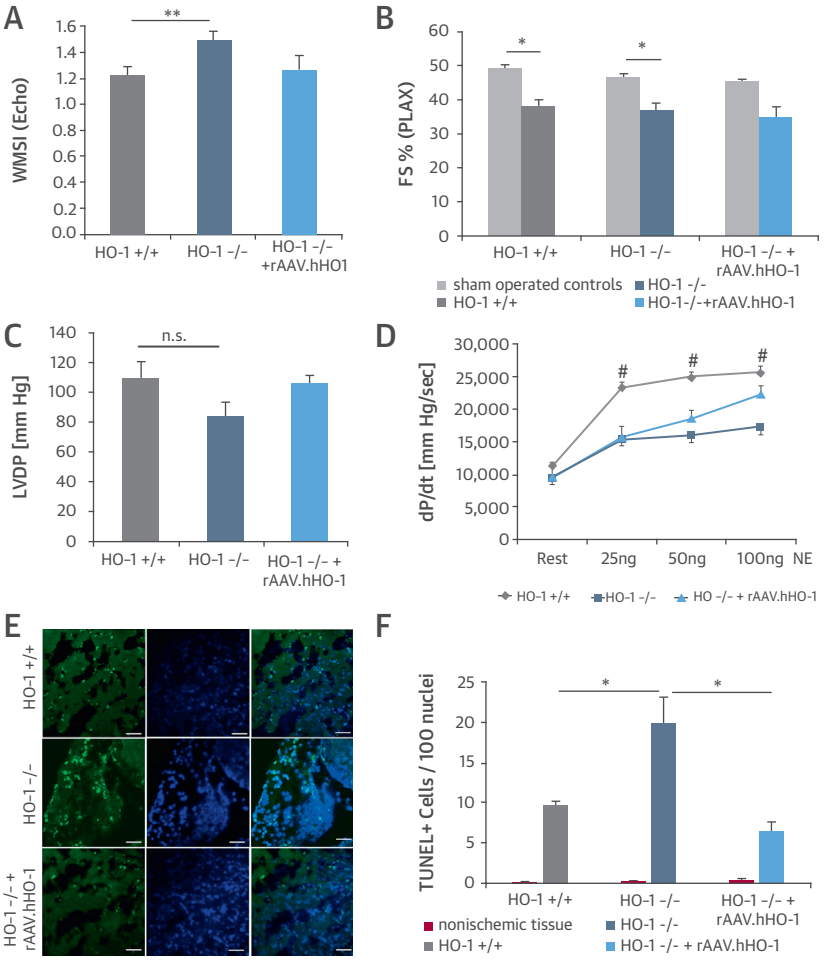

(A) Echocardiography revealed an increased wall motion score index (WMSI), indicating an increase in infarct size, in HO-1-deficient mice, but without a significant difference **(B)** in post-ischemic loss of ejection fraction (**grey column**, sham-operated mice). **(C)** Invasive hemodynamic analysis (Millar tip catheter) revealed similar left ventricular developed pressures (LVDPs) in all groups at rest. **(D)** An impaired contraction velocity (dP/dt_{max}) following norepinephrine (NE) bolus stimulation was partially restored by rAAV.hHO-1 application. Examples **(E)** and analysis **(F)** showed that TUNEL-positive cells were found more frequently in the infarcted area of HO-1-deficient mice. Scale bar = 50 μm. Mean ± standard error of the mean; n = 7; *p < 0.05, **p < 0.005, #p < 0.05 vs. HO-$1^{-/-}$. FS = fractional shortening; I/R = ischemia and reperfusion; PLAX = parasternal long axis; TUNEL = deoxynucleotidyltransferase dUTP nick end labeling; other abbreviations as in **Figures 1 and 2**.

(**Figure 2B**). Consistently, homozygous HO-1-deficient hearts recruited more Ly-6G-positive neutrophils (7.1 ± 1.3 × 10^3 cells/mg) than control and heterozygous hearts (1.0 ± 0.2 × 10^3 and 3.0 ± 0.6 × 10^3 cells/mg, respectively) (**Figure 2C**). This pattern was replicated for proinflammatory Ly-$6C^{high}$ monocytes (3.0 ± 0.6 × 10^3 cells/mg) but not heterozygous (1.2 ± 0.2 × 10^3 cells/mg) and control siblings (0.8 ± 0.3 × 10^3 cells/mg) (**Figure 2D**). In contrast, no significant difference was found when we analyzed Ly-$6C^{low}$ proangiogenic monocytes (**Figure 2E**). Of note, rAAV transduction of hHO-1 in HO-1-deficient mice attenuated the increased recruitment of CD45.2, $CD11b^+$, Ly-6G, and Ly-$6C^{high}$ cells (**Figures 2A to 2D**). Moreover, rAAV.hHO-1 reduced Ly-6G and increased Ly-$6C^{low}$ cells in wild-type mice, compared with rAAV.GFP (Online Figures 3A to 3F). Taken together, HO-1 deficiency increased post-ischemic inflammation, in particular of neutrophil and Ly-$6C^{high}$ monocytic cell infiltration.

FIGURE 4 hHO-1 Affects Post-Ischemic Inflammation

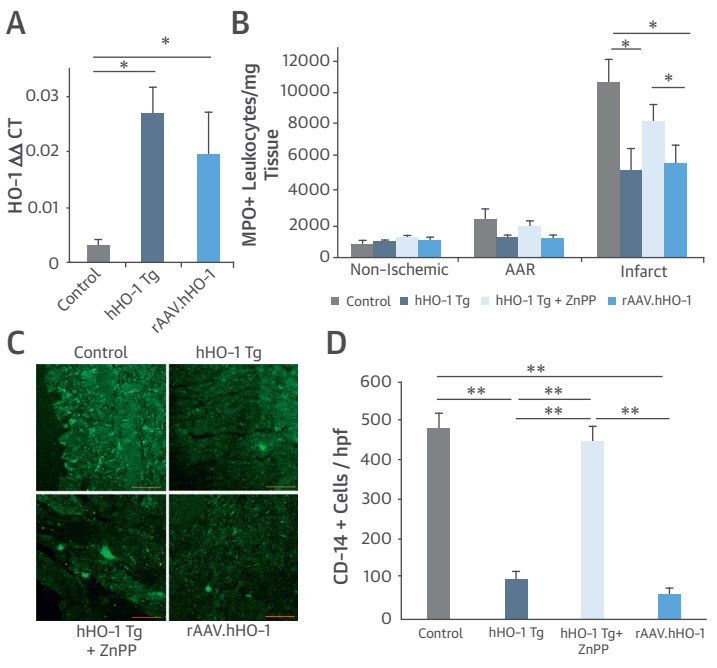

(A) Quantitative real-time polymerase chain reaction analysis of hHO-1 expression showed a significant increase of hHO-1 in hHO-1 transgenic (hHO-1.tg) as well as in rAAV.hHO-1-treated pigs (n = 3 per group). **(B)** Recruitment of myeloperoxidase-positive (MPO^+) leukocytes to the infarct area was significantly increased in the infarct region of control animals. hHO-1.tg pigs displayed an attenuated leukocyte recruitment, unless ZnPP was coapplied. Transduction of cardiomyocytes with rAAV.hHO-1 mimicked the effect of hHO-1 transgenic hearts. **(C)** Examples of $CD14^+$ macrophages in the noninfarcted area at risk of control and hHO-1 transgenic animals. **(D)** Quantitative analysis revealed a significant decrease of $CD14^+$ cells/hpf in hHO-1.tg and rAAV.hHO-1 transduced hearts, unless ZnPP was coapplied. Scale bar = 50 μm. Mean ± standard error of the mean; n = 5; *p < 0.05, **p < 0.001. Abbreviations as in Figures 1 and 2.

Consistently, assessing hypokinetic or akinetic areas with an echocardiographic WMSI (19,29) demonstrated an increase in infarct size in HO-1-deficient mice (Figure 3A), which was not detectable in 2-dimensional echocardiography (Figure 3B) or in pinhole single-photon emission computerized tomography analysis (Online Figures 3G and 3H). Interestingly, rAAV.hHO-1 application increased post-ischemic EF in wild-type mice compared with rAAV.GFP (Online Figure 3F). In contrast, invasive assessment of LV pressure did not reveal a significant decrease in HO-1-deficient hearts at rest, with or without rAAV.hHO-1 application (Figure 3C). An additional challenge of the hearts with increasing amounts of norepinephrine (25 to 100 ng boli intravenously) unmasked a lack of contractile responsiveness in $HO\text{-}1^{-/-}$ hearts (Figure 3D), which was attenuated by rAAV.hHO-1 application. Consistent with these results, terminal deoxynucleotidyl-transferase dUTP nick end labeling-positive nuclei were found at higher rates in HO-1-deficient mouse hearts (Figures 3E and 3F). Of note, TLR4 deficiency did not alter functional impairment significantly (Online Figure 4). Thus, in the absence of HO-1, we found a small but significant impairment of myocardial infarct size, which did not affect myocardial function at rest but decreased functional LV reserve under adrenergic stimulation.

We next analyzed the effect of HO-1 on post-ischemic inflammation in pigs, subjecting porcine hearts to 1 h of ischemia (LAD occlusion) followed by 24 h of reperfusion. In addition to transgenic pigs overexpressing human HO-1, we applied an AAV encoding for hHO-1 (rAAV.hHO-1) with a similar hHO-1 expression level (Figure 4A, Online Figure 1B) or an rAAV.LacZ control vector via retroinfusion.

Compared with the normoxic region and the non-infarcted AAR, a massive influx of MPO^+ neutrophils was observed in the infarct area ($10.1 \pm 1.3 \times 10^3$ vs. $0.8 \pm 0.1 \times 10^3$ cells/mg normoxic area, $2.1 \pm 0.7 \times 10^3$ cells/mg AAR) (Figure 4B, Online Figure 5). Overexpression of hHO-1 in transgenic animals significantly reduced the recruitment of MPO^+ cells ($4.7 \pm 1.3 \times 10^3$ cells/mg), whereas HO-1 inhibition (ZnPP) reset the level of MPO^+ cells in the infarct zone to that of wild-type animals ($10.3 \pm 0.9 \times 10^3$ cells/mg). Of note, regional treatment of the ischemic myocardium with rAAV.hHO-1 sufficed to reduce the MPO^+ cell influx by 46% ($5.3 \pm 1.1 \times 10^3$ cells/mg) (Figure 4B). Accordingly, proinflammatory $CD14^+$ monocytes were accumulating in the infarcted area (480 ± 39 cells/mm^2) of wild-type hearts (Figures 4C and 4D). This effect was largely reduced by hHO-1 overexpression: in rAAV.hHO-1-treated hearts, we found 61 ± 16 cells/mm^2 and in hHO-1.tg hearts 98 ± 20 cells/mm^2, unless ZnPP was coapplied (453 ± 37 cells/mm^2) (Figures 4C and 4D).

Ischemic and inflammatory processes inflict abrogation of functional capillaries in the ischemic area. Because microvascular density is closely correlated to residual post-ischemic function, we analyzed capillary densities in the infarct border zone. In rAAV.hHO-1 and HO-1.tg hearts, the level of $CD31^+$ capillaries was more than double that of control hearts (Online Figures 6A and 6B), unless the HO-1 inhibitor ZnPP was added to hHO-1.tg hearts. This effect might still be initiated by hHO-1-transduced cardiomyocytes, because the conditioned medium of hHO-1-transfected cardiomyocytic HL-1 cells increased endothelial cell survival after

FIGURE 5 hHO-1 Affects Infarct Size in Porcine Ischemia-Reperfusion

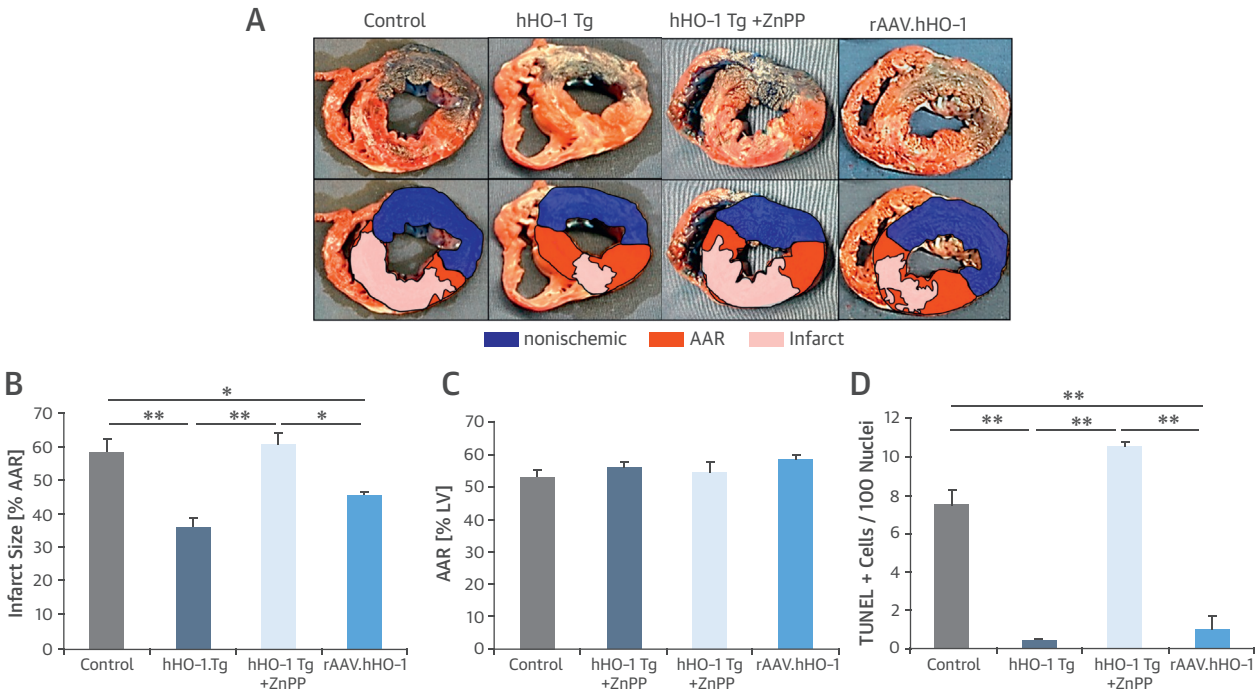

(A) Examples of heart samples stained with methylene blue in the nonischemic area and with triphenyltetrazolium chloride in the ischemic left anterior descending coronary artery–perfused area at risk (AAR; **red** = vital area, **pale** = avital area). **(B)** Quantitative analysis of the infarct size in pigs revealed a significant reduction of the infarct in the hHO-1.tg and rAAV.hHO-1-treated animals, an effect eliminated after ZnPP application. **(C)** AAR of the left ventricle did not differ between the groups. **(D)** TUNEL-positive cardiac cells were found decreased in rAAV.hHO-1 and hHO-1.tg hearts, unless ZnPP was applied to inhibit HO-1. Mean ± standard error of the mean; n = 5; *p < 0.05, **p < 0.001. LV = left ventricular; other abbreviations as in Figures 1, 2, and 3.

hypoxia/reoxygenation, a surrogate parameter for capillary preservation after I/R in vivo (Online Figures 6C and 6D).

In this model, infarct size of control hearts (55 ± 5% AAR) was significantly reduced by rAAV.hHO-1 retroinfusion (41 ± 3%), similar to hHO-1.tg pigs (35 ± 4%) (**Figures 5A and 5B**). Consistently, the cardioprotection of hHO-1.tg pigs was reversed by regional application of the specific HO-1 inhibitor ZnPP (61 ± 3% infarct size) (**Figures 5A and 5B**). The AAR of these groups did not differ in our study (**Figure 5C**). Of note, terminal deoxynucleotidyltransferase dUTP nick end labeling-positive cell death was significantly reduced in the hHO-1-overexpressing pigs at 24 h, unless HO-1 was inhibited by ZnPP (**Figure 5D**). In particular, cardiomyocyte and endothelial apoptosis was prevented by hHO-1 (Online Figure 7).

According to the structural impact of our I/R protocol, the difference between pre- and post-ischemic LVEF varied significantly, although the pre-ischemic levels did not vary among groups (Online Figure 8A). In rAAV.LacZ-treated control animals, change in EF was 28 ± 3% (**Figure 6A**). This I/R-induced loss of function was attenuated in both hHO-1-overexpressing groups, either rAAV.hHO1-treated (17 ± 2%) or hHO-1.tg pigs (16 ± 2%). However, retroinfusion of the HO-1 inhibitor ZnPP abrogated the functional benefit of hHO-1.tg pigs (27 ± 2%). Similarly, the post-ischemic increase in change in EF and LV end-diastolic pressure (3.1 ± 0.6 mm Hg in control animals) decreased to 0.3 ± 0.5 mm Hg (hHO-1.tg) and 1.1 ± 0.5 mm Hg (rAAV.hHO-1). The latter effect was reversed by ZnPP (3.8 ± 0.6 mm Hg) (**Figure 6B**, Online Figure 8B).

This improvement in global systolic function was mirrored in regional myocardial function of non-infarcted AAR. Here, rAAV.LacZ-treated control hearts displayed 25 ± 5% of the myocardial shortening in the nonischemic control region at rest, worsening to akinesia (2 ± 4%) under the challenge of rapid atrial pacing (150 min) (**Figure 6C**). Human

FIGURE 6 Functional Impact of hHO-1

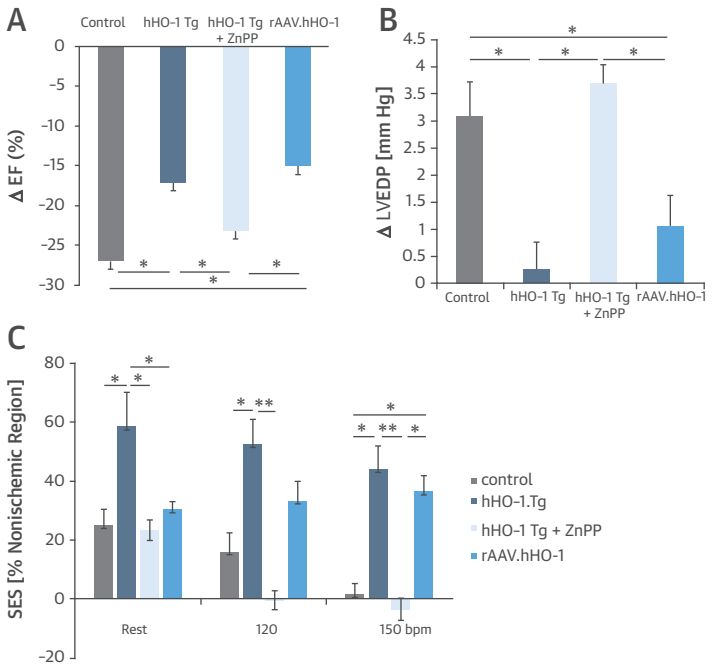

(A) Analysis of left ventricular function revealed a loss of ejection fraction (EF) after I/R in control hearts, which was attenuated in animals with enhanced HO-1 levels (hHO-1.tg and rAAV.hHO-1). ZnPP abolished the cardioprotective effect of hHO-1.tg. **(B)** Left ventricular end-diastolic pressure (LVEDP) increased in control hearts, but not in hHO-1-supplied hearts (hHO-1.tg and rAAV.hHO-1). ZnPP blocked the effect in hHO-1.tg hearts. **(C)** Regional myocardial function of the infarct area was assessed by subendothelial sonomicrometry (SES) at rest and rapid atrial pacing (120 and 150 bpm). hHO-1.tg and rAAV.hHO-1 treated hearts displayed preserved regional myocardial function at higher heart rates, as opposed to rAAV.LacZ-treated control hearts or hHO-1.tg +ZnPP treated hearts. Mean ± standard error of the mean; n = 5; *p < 0.05, **p < 0.001. bpm = beats per minute; LacZ = ß-galactosidase; other abbreviations as in Figures 1, 2, and 3.

HO-1.tg hearts demonstrated a significant higher preservation of functional reserve at rest (58 ± 5%) as well as under atrial pacing of 150 beats/min (44 ± 8%). Antagonizing HO-1 via ZnPP blocked the increase in regional myocardial function of hHO-1.tg pig hearts (−3 ± 4%). Of note, rAAV.hHO-1 transduction, displaying no difference to control hearts at rest, significantly increased regional myocardial function at 150 beats/min (37 ± 5%). Thus, exogenous supply of hHO-1 to cardiomyocytes reduces cellular damage and death and protects post-ischemic function. Taken together, an enhanced abundance of HO-1 in hHO-1.tg hearts and rAAV.HO-1-transduced hearts seems to improve cardiomyocyte survival and function. Both coincide with attenuation of post-ischemic inflammation and improved microvessel preservation.

DISCUSSION

Recently, inflammatory events have been scrutinized for their impact on cardiac I/R injury. Besides the composition and origin of invading inflammatory cells (6), the amount of cells and the kinetics of their recruitment seem to determine the expansion of the fibrotic scar and the cardiac remodeling accompanying its establishment (30). Therefore, we asked whether HO-1, known for its immunomodulatory properties in cell culture (31,32) and in xenotransplantation (22,33), is capable of altering the post-ischemic immune response and subsequent functional outcome in cardiac I/R injury.

In vitro, HO-1 suffices to blunt inflammatory activation of endothelial cells in culture, thereby limiting their potential to recruit inflammatory monocytes under flow conditions (Figure 1). In vivo, post-ischemic inflammatory cell influx increased in HO-1-deficient mice: neutrophilic Ly-6G^{+} and proinflammatory monocytic Ly-6G^{high} subsets were recruited at higher rates to murine hearts after 45 min of ischemia and 24 h of reperfusion, when HO-1 was absent (Figure 2). Moreover, LV wall motion, functional reserve, and apoptosis were all impaired in HO-1$^{-/-}$ animals (Figure 3).

In porcine I/R studies, ubiquitous transgenic overexpression and regional AAV transduction of HO-1 both achieved similar levels of inflammation control (Figure 4), consistent with decreased infarct size (Figure 5) and improved LV function (Figure 6). Of note, the recombinant AAV2/9 regionally applied in this study primarily targets cardiomyocytes (34,35), with minimal contamination of endothelial cells or macrophages found in tomato reporter gene mice (data not shown). This observation carries the implication that rAAV.HO-1-based gene therapy mainly targets intracardiac processes that initiate recruitment of neutrophils and inflammatory monocytes as well as functional impairment. In contrast, additional effects of HO-1 on extracardiac targets (e.g., in circulating leukocytes of the transgenic, ubiquitously HO-1-overexpressing pigs) do not seem essential for HO-1-mediated cardioprotection.

This argues for a central relevance of the myocardium itself as target of HO-1-mediated cardioprotection and origin of post-ischemic inflammatory signaling, and renders endothelial protection and angiogenesis as secondary processes. We consistently observed a distinct anti-inflammatory effect of HO-1 in both models of I/R. We followed a potential

CENTRAL ILLUSTRATION **HO-1 Gene Therapy Provides Cardioprotection in Porcine Ischemic Reperfusion**

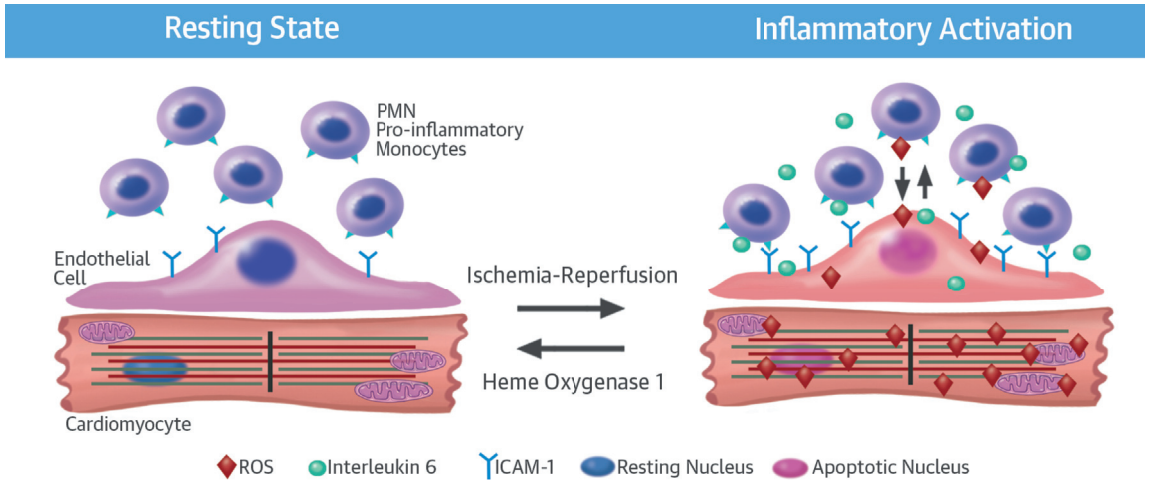

Hinkel, R. et al. J Am Coll Cardiol. 2015; 66(2):154–65.

A resting state is defined by low ROS and an anti-adhesive, inactive endothelium. Inflammatory activation induces ROS production, chemokine and adhesion molecule upregulation, leukocyte recruitment, and apoptosis. Heme oxygenase-1 (HO-1) is capable of reversing inflammatory activation toward the resting state. ICAM = intercellular adhesion molecule; PMN = polymorphonuclear neutrophils; ROS = reactive oxygen species.

interaction of HO-1 with TLR4 (36,37), a receptor for damage-associated molecular patterns, such as high mobility group box 1 (38). the latter being released from ischemic cardiomyocytes (39). However, neither inflammatory cell influx nor function was significantly altered in TLR4-deficient mice in our I/R model (Online Figure 4).

In the porcine model, the functional impact in hHO-1-constrained post-ischemic inflammation was already apparent at rest (**Central Illustration**), whereas in HO-1$^{-/-}$ mice functional impairment was unmasked solely on adrenergic stimulation. Of note, diabetes mellitus, which inflicts chronic vascular inflammation, further exacerbates infarct size in HO-1-deficient mice in a 60-min LAD occlusion model (40). We could obtain an increased infarct size only with the sensitive WMSI (**Figure 3A**), but not with pinhole single-photon emission computerized tomography measurement (20) (Online Figures 3G and 3H), most likely because of a limited spatial resolution of 1.9 mm. Accordingly, hHO-1.tg mice display infarct size reduction after 60 min of ischemia (14), similar to our porcine models of hHO-1 overexpression (**Figure 5**). Besides the time sensitivity, structural differences, regional application of the rAAV.hHO-1 vector, and a more neutrophil-prone immune system, with 11-25G/l neutrophils circulating in blood without inflammatory stimulation, may have contributed to a more robust hHO-1 effect in the porcine model.

The anti-inflammatory potential of HO-1 has previously been revealed in heart transplantation (41), although that adaptive immune reaction differs from innate immune reactivity in post-ischemic inflammation. For the latter, the composition of leukocyte influx is of particular interest, because a well-orchestrated sequence of proinflammatory and anti-inflammatory events takes place in post-ischemic cardiac repair: neutrophil and proinflammatory Ly-6C^{high} monocytes catabolize cell debris and pave new avenues for anti-inflammatory, proangiogenic Ly-6C^{low} monocytes and myofibroblasts to form a residual tissue wall and provide blood supply therein. However, current reperfusion therapies may overwhelm the heart with leukocyte influx via the infarct artery, an avenue permanently occluded in the natural disease course (9). This early proinflammatory cell influx is reduced when HO-1 is overexpressed, improving functional outcome in the porcine model. In contrast, regenerative monocyte recruitment was unaffected by modulation of HO-1 (**Figure 2**).

STUDY LIMITATIONS. Although we have demonstrated successful treatment of I/R injury in a preclinical porcine model, we are aware that the use of young, healthy animals does not necessarily reflect the treatment efficacy in elderly, cardiovascular risk-factor exposed patients. Moreover the pre-treatment

with recombinant AAV vector as conducted in this study does not cover its application as adjuvant therapy in the treatment of acute myocardial infarction, where rapid activation of HO-1 may require a different approach.

CONCLUSIONS

We have demonstrated that HO-1 overexpression limits proinflammatory activation of ischemia-challenged cardiomyocytes and inflammatory cell influx in reperfused murine and porcine hearts. Enhancing HO-1 activity in early reperfusion improves post-ischemic function in a pre-clinical pig model and seems a suitable approach to treat post-I/R injury.

ACKNOWLEDGMENTS The authors thank Elisabeth Raatz and Cuong Kieu for expert technical assistance.

REPRINT REQUESTS AND CORRESPONDENCE: Dr. Christian Kupatt, I. Medizinische Klinik und Poliklinik, Klinikum Rechts der Isar, TUM, Ismaningerstrasse 22, Munich, Germany 81675. E-mail: christian.kupatt@tum.de.

PERSPECTIVES

COMPETENCY IN MEDICAL KNOWLEDGE: HO-1 attenuates post-ischemic cardiac inflammation, and regional rAAV-encoding human HO-1 gene therapy improves ventricular ejection fraction in animal models.

TRANSLATIONAL OUTLOOK: Further studies are needed to determine whether strategies that activate HO-1 might have clinical value for prevention or treatment of ischemia-reperfusion injury in the human heart.

REFERENCES

1. Hao K, Hanawa H, Ding L, et al. Free heme is a danger signal inducing expression of proinflammatory proteins in cultured cells derived from normal rat hearts. Mol Immunol 2011;48:1191–202.

2. Ryter SW, Alam J, Choi AMK. Heme oxygenase-1/carbon monoxide: from basic science to therapeutic applications. Physiol Rev 2006;86:583–650.

3. Liu X, Simpson JA, Brunt KR, et al. Preemptive heme oxygenase-1 gene delivery reveals reduced mortality and preservation of left ventricular function 1 yr after acute myocardial infarction. Am J Physiol Heart Circ Physiol 2007;293:H48–59.

4. Pachori AS, Melo LG, Zhang L, Solomon SD, Dzau VJ. Chronic recurrent myocardial ischemic injury is significantly attenuated by pre-emptive adeno-associated virus heme oxygenase-1 gene delivery. J Am Coll Cardiol 2006;47:635–43.

5. Wang G, Hamid T, Keith RJ, et al. Cardioprotective and antiapoptotic effects of heme oxygenase-1 in the failing heart. Circulation 2010;121:1912–25.

6. Nahrendorf M, Swirski FK, Aikawa E, et al. The healing myocardium sequentially mobilizes two monocyte subsets with divergent and complementary functions. J Exp Med 2007;204:3037–47.

7. Liu X, Pachori AS, Ward CA, et al. Heme oxygenase-1 (HO-1) inhibits postmyocardial infarct remodeling and restores ventricular function. FASEB J 2006;20:207–16.

8. Timmers L, Pasterkamp G, de Hoog VC, Arslan F, Appelman Y, de Kleijn DP. The innate immune response in reperfused myocardium. Cardiovasc Res 2012;94:276–83.

9. Frangogiannis NG. Regulation of the inflammatory response in cardiac repair. Circ Res 2012;110:159–73.

10. Epelman S, Liu PP, Mann DL. Role of innate and adaptive immune mechanisms in cardiac injury and repair. Nat Rev Immunol 2015;15:117–29.

11. Wantha S, Alard JE, Megens RTA, et al. Neutrophil-derived cathelicidin promotes adhesion of classical monocytes. Circ Res 2013;112:792–801.

12. Libby P, Nahrendorf M, Swirski FK. Monocyte heterogeneity in cardiovascular disease. Semin Immunopathol 2013;35:553–62.

13. Seropian IM, Toldo S, Van Tassell BW, Abbate A. Anti-inflammatory strategies for ST-elevation acute myocardial infarction ventricular remodeling. J Am Coll Cardiol 2014;63:1593–603.

14. Yet SF, Tian R, Layne MD, et al. Cardiac-specific expression of heme oxygenase-1 protects against ischemia and reperfusion injury in transgenic mice. Circ Res 2001;89:168–73.

15. Zhao Y, Zhang L, Qiao Y, et al. Heme oxygenase-1 prevents cardiac dysfunction in streptozotocin-diabetic mice by reducing inflammation, oxidative stress, apoptosis and enhancing autophagy. PLoS One 2013;8:e75927.

16. Xue J, Habtezion A. Carbon monoxide-based therapy ameliorates acute pancreatitis via TLR4 inhibition. J Clin Invest 2014;124:437–47.

17. Bish LT, Morine K, Sleeper MM, et al. AAV9 provides global cardiac gene transfer superior to AAV1, AAV6, AAV7, and AAV8 in the mouse and rat. Hum Gene Ther 2008;19:1359–68.

18. Yet SF, Perrella MA, Layne MD, et al. Hypoxia induces severe right ventricular dilatation and infarction in heme oxygenase-1 null mice. J Clin Invest 1999;103:R23–9.

19. Zhang Y, Takagawa J, Sievers RE, et al. Validation of the wall motion score and myocardial performance indexes as novel techniques to assess cardiac function in mice after myocardial infarction. Am J Physiol Heart Circ Physiol 2007;292:H1187–92.

20. Wollenweber T, Zach C, Rischpler C, et al. Myocardial perfusion imaging is feasible for infarct size quantification in mice using a clinical single-photon emission computed tomography system equipped with pinhole collimators. Mol Imaging Biol 2010;12:427–34.

21. Horstkotte J, Perisic T, Schneider M, et al. Mitochondrial thioredoxin reductase is essential for early postischemic myocardial protection. Circulation 2011;124:2892–902.

22. Petersen B, Ramackers W, Lucas-Hahn A, et al. Transgenic expression of human heme oxygenase-1 in pigs confers resistance against xenograft rejection during ex vivo perfusion of porcine kidneys. Xenotransplantation 2011;18:355–68.

23. Kupatt C, Hinkel R, von Bruhl ML, et al. Endothelial nitric oxide synthase overexpression provides a functionally relevant angiogenic switch in hibernating pig myocardium. J Am Coll Cardiol 2007;49:1575–84.

24. Kupatt C, Hinkel R, Pfosser A, et al. Cotransfection of vascular endothelial growth factor-A and platelet-derived growth factor-B via recombinant adeno-associated virus resolves chronic ischemic malperfusion: role of vessel maturation. J Am Coll Cardiol 2010;56:414–22.

25. Hinkel R, Penzkofer D, Zuehlke S, et al. Inhibition of microRNA-92a protects against ischemia-reperfusion injury in a large animal model. Circulation 2013;128:1066–75.

26. Hinkel R, El-Aouni C, Olson T, et al. Thymosin ß 4 is an essential paracrine factor of embryonic

endothelial progenitor cell-mediated cardioprotection. Circulation 2008;117:2232–40.

27. Kupatt C, Hinkel R, Lamparter M, et al. Retroinfusion of embryonic endothelial progenitor cells attenuates ischemia-reperfusion injury in pigs: role of phosphatidylinositol 3-kinase/AKT kinase. Circulation 2005;112 Suppl: I117–22.

28. Kupatt C, Wichels R, Horstkotte J, Krombach F, Habazettl H, Boekstegers P. Molecular mechanisms of platelet-mediated leukocyte recruitment during myocardial reperfusion. J Leukoc Biol 2002;72: 455–61.

29. Takagawa J, Zhang Y, Wong ML, et al. Myocardial infarct size measurement in the mouse chronic infarction model: comparison of area- and length-based approaches. J Appl Physiol 2007; 102:2104–11.

30. Leuschner F, Rauch PJ, Ueno T, et al. Rapid monocyte kinetics in acute myocardial infarction are sustained by extramedullary monocytopoiesis. J Exp Med 2012;209:123–37.

31. Seldon MP, Silva G, Pejanovic N, et al. Heme oxygenase-1 inhibits the expression of adhesion molecules associated with endothelial cell activation via inhibition of NF-kappaB RelA phosphorylation at serine 276. J Immunol 2007;179: 7840–51.

32. Chabannes D, Hill M, Merieau E, et al. A role for heme oxygenase-1 in the immunosuppressive effect of adult rat and human mesenchymal stem cells. Blood 2007;110:3691–4.

33. Soares MP, Lin Y, Anrather J, et al. Expression of heme oxygenase-1 can determine cardiac xenograft survival. Nat Med 1998;4:1073–7.

34. Pleger ST, Shan C, Ksienzyk J, et al. Cardiac AAV9-S100A1 gene therapy rescues post-ischemic heart failure in a preclinical large animal model. Sci Transl Med 2011;3:92ra64.

35. Asokan A, Samulski RJ. An emerging adeno-associated viral vector pipeline for cardiac gene therapy. Hum Gene Ther 2013;24:906–13.

36. Wang XM, Kim HP, Nakahira K, Ryter SW, Choi AMK. The heme oxygenase-1/carbon monoxide pathway suppresses TLR4 signaling by regulating the interaction of TLR4 with caveolin-1. J Immunol 2009;182:3809–18.

37. Mandal P, Roychowdhury S, Park PH, Pratt BT, Roger T, Nagy LE. Adiponectin and heme oxygenase-1 suppress TLR4/MyD88-independent signaling in rat Kupffer cells and in mice after chronic ethanol exposure. J Immunol 2010;185:4928–37.

38. Li G, Tang D, Lotze MT. Menage a trois in stress: DAMPs, redox and autophagy. Semin Cancer Biol 2013;23:380–90.

39. Andrassy M, Volz HC, Igwe JC, et al. High-mobility group box-1 in ischemia-reperfusion injury of the heart. Circulation 2008;117:3216–26.

40. Liu X, Wei J, Peng DH, Layne MD, Yet SF. Absence of heme oxygenase-1 exacerbates myocardial ischemia/reperfusion injury in diabetic mice. Diabetes 2005;54:778–84.

41. Ma J, Lau CK, Obed A, et al. A cell penetrating heme oxygenase protein protects heart graft against ischemia/reperfusion injury. Gene Ther 2009;16:320–8.

KEY WORDS adenoassociated virus, cardiomyocyte, endothelial, reperfusion, transgenic

APPENDIX For supplemental figures, please see the online version of this article.